



Communication

An Innovative Design of Isoflux Scanning Digital Phased Array Based on Completely Shared Subarray Architecture for Geostationary Satellites

Muren Cai ^{1,2,*} , Wentao Li ¹, Xiaowei Shi ¹, Qiaoshan Zhang ², Heng Liu ² and Yan Li ² 

¹ Department of Electronic Engineering, Xidian University, Xi'an 710071, China; liwentao_xa@163.com (W.L.); xwshi@mail.xidian.edu.cn (X.S.)

² China Academy of Space Technology (Xi'an), Xi'an 710000, China; zhangqs_504@163.com (Q.Z.); liuheng@mail.nankai.edu.cn (H.L.); liyaanem@gmail.com (Y.L.)

* Correspondence: mr_cai2012@126.com

Abstract: In this paper, we propose an innovative spaceborne isoflux scanning digital phased array (ISDPA) design with two-stage digital beamforming (DBF) for geostationary satellites. To achieve isoflux scanning, a novel technique is presented to obtain an isoflux beam for the ISDPA equivalent element using a DBF completely shared subarray architecture and the differential evolution (DE) algorithm. By reutilizing the radiating elements of adjacent subarrays, the radiation aperture and element number are augmented, enhancing the degrees of optimization freedom. To validate the proposed design, a linear ISDPA with 16 DBF completely shared subarrays is optimized and analyzed using two sets of excitation coefficients in different DBF stages. The numerical results demonstrate that the proposed ISDPA can adaptively compensate for space loss variations during beam scanning for geostationary communications with low sidelobes better than -20 dB.

Keywords: phased array antenna; isoflux scanning; shared subarray; digital beamforming; space loss; geostationary satellites



Citation: Cai, M.; Li, W.; Shi, X.; Zhang, Q.; Liu, H.; Li, Y. An Innovative Design of Isoflux Scanning Digital Phased Array Based on Completely Shared Subarray Architecture for Geostationary Satellites. *Electronics* **2023**, *12*, 3850. <https://doi.org/10.3390/electronics12183850>

Academic Editor: Manuel García Sanchez

Received: 30 July 2023

Revised: 4 September 2023

Accepted: 8 September 2023

Published: 12 September 2023



Copyright: © 2023 by the authors. Licensee MDPI, Basel, Switzerland. This article is an open access article distributed under the terms and conditions of the Creative Commons Attribution (CC BY) license (<https://creativecommons.org/licenses/by/4.0/>).

1. Introduction

Satellite communication systems play a crucial role in a wide range of applications, including mobile communications, global emergency services, and broadcasting services [1,2]. Today, satellites are commonly utilized for transmitting various types of information, including data, voice, and video [3,4]. Due to this fact, a satellite for the space segment can require different kinds of antennas serving as transducers that convert electromagnetic energy for either receiving or transmitting signals. Phased array antennas are increasingly attractive and widely adopted in satellite payloads due to their advantageous features, including high beam agility, high gain, multi-beams, and flexible pattern beamforming [5–7]. It is widely acknowledged that space loss is minimal at the nadir position, where the shortest path exists between the satellite and the ground user. However, space loss increases as the ground target moves away from the nadir. To compensate for changing path loss between users at different locations on the Earth and satellites, a kind of spaceborne phased array antenna with isoflux scanning characteristics is needed to provide a consistent satellite communication link to any point of the illuminated Earth surface during beam scanning.

There are many studies for antennas that have isoflux radiation characteristics in the literature [8–15]. Volkan Akan presented a polyrod antenna that has an isoflux radiation characteristic for satellite communication systems in [8]. In this study, the polyrod antenna was a single antenna with fixed isoflux coverage. E. Arnaud suggested a compact isoflux X-band payload telemetry and data-handling antenna with simultaneous dual circular polarization for low-Earth orbit (LEO) satellite applications [9]. This antenna relies on a choke horn, a conventional septum polarizer, and a dielectric cone with a particular

shape at an open-ended waveguide to generate the isoflux radiation pattern. F. Caminita presented a low-profile dual-polarized isoflux antenna based on an artificial impedance surface realized by means of printed metallic strips and metallic corrugations at the X-band for space applications [10]. This isoflux antenna is a single antenna with an aperture of 13λ (λ is the wavelength of operating frequency). Furthermore, a planar metasurface isoflux-type antenna based on an anisotropic metasurface with an isoflux pattern for LEO satellite application was proposed in [11]. Moreover, isoflux radiation patterns can be obtained via the array antenna. In the study of [12], the design of an aperiodic array for isoflux radiation was reported. This isoflux array considered the reduction in the sidelobe level and the isoflux radiation requirements for geostationary Earth orbit (GEO) satellites by utilizing the method of genetic algorithms. The study of [13] reported an isoflux microstrip array at the X band with applications in Cubesat communications. The isoflux array was chosen to be a set of concentric ring elements and was designed by using a genetic algorithm to obtain appropriate elements, such as spacing, amplitude, and phase shifts, for isoflux radiation pattern optimization. Another isoflux antenna for Cubesat applications was presented in [14], consisting of three concentric annular apertures to obtain an isoflux beam pattern. The study of [15] presented an isoflux thinned array for GEO satellites using the Fourier series synthesis method. Nevertheless, all the isoflux beam antennas above exhibit fixed coverages and were, thus, unable to achieve flexible and fast beam steering.

This paper proposes an innovative isoflux scanning digital phased array antenna (ISDPA) design for GEO satellite payloads with a scanning range of -8° to 8° . Since optimizing the radiation pattern variation in phased array elements within the scanning range is crucial for controlling scanning gain variation, this paper also presents a novel method to achieve an isoflux-shaped beam for the equivalent element of the ISDPA. This is accomplished by utilizing a completely shared subarray architecture and differential evolution (DE) algorithm. The radiation aperture can be shared between adjacent subarrays, which increases the aperture size and number of elements in the digital shared subarray. Thus, the challenges related to isoflux radiation pattern beam shaping can be greatly mitigated due to improved degrees of optimization freedom. Specifically, the ISDPA reaches minimum gain at nadir without scanning. As the beam scanning angle increases, the gain rises accordingly, providing effective compensation for link loss resulting from the path loss variation during beam scanning, demonstrating the isoflux scanning characteristic. Additionally, the proposed ISDPA design achieves low sidelobe levels.

The main contribution of this communication is summarized as follows:

- (1) This work proposes a solution for a spaceborne phased array antenna to equalize flux density across the ground coverage during electrical beam scanning, which has not been presented until now to the best of the authors' knowledge;
- (2) Through the digital signal multiplexing and combination after analog-to-digital conversion in digital beamforming, the complexity of physically implementing the shared subarray architecture is greatly simplified;
- (3) Through numerical optimization, the scanning gain variation in the phased array antenna closely matches the space attenuation variation during beam scanning in GEO satellite communications.

2. Design of the ISDPA

2.1. Scheme of the ISDPA Based on the DBF Completely Shared Subarray

The shared subarray architecture has been utilized in limited scan arrays [16], where scanning at the subarray level suppresses grating lobes and reduces sidelobes. In this architecture, sharing antenna elements between adjacent subarrays increases the radiation aperture and the number of elements, facilitating beam shaping [17,18]. Similarly, the digital beamforming (DBF) completely shared subarray structure can utilize extra radiating elements for subarray beamforming. As illustrated in Figure 1a, the linear DBF completely shared subarray with N elements consists of radiating elements, low-noise amplifiers (LNAs), frequency converters, A/D converters, and the first-stage digital beamforming

network. Each element’s aperture is shared across all subarrays, meaning each element participates in digital beamforming via the first-stage DBF processor of every shared subarray. The element spacing and the shared subarray phase center spacing are both d . A linear N -element DBF completely shared subarray with array geometry is shown in Figure 1b, where $A_i^{(1)}$ denotes the excitation coefficient of the i th element for the first-stage DBF, $f(\theta)$ is the element pattern, and the completely shared subarray pattern $F(\theta)$ can be obtained as:

$$F(\theta) = \sum_{i=1}^n A_i^{(1)} e^{j(kid \sin \theta + \varphi_i)} f(\theta) = AF^{(1)}(\theta) \times f(\theta) \tag{1}$$

where $AF^{(1)}(\theta)$ is the subarray factor at the radiating element level, and $k = 2\pi/\lambda$ is the free-space wavenumber.

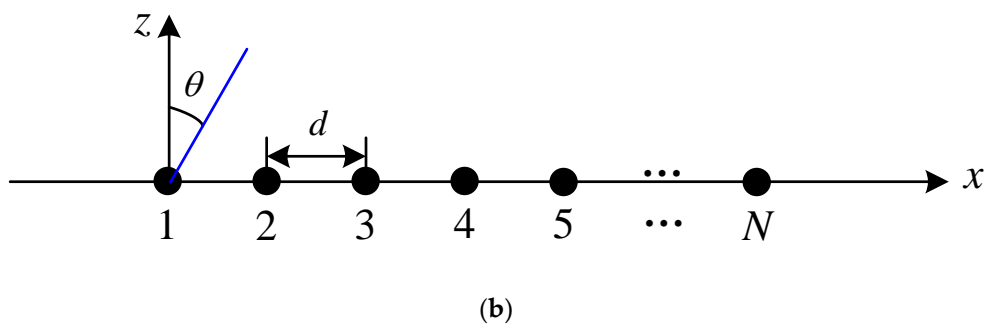
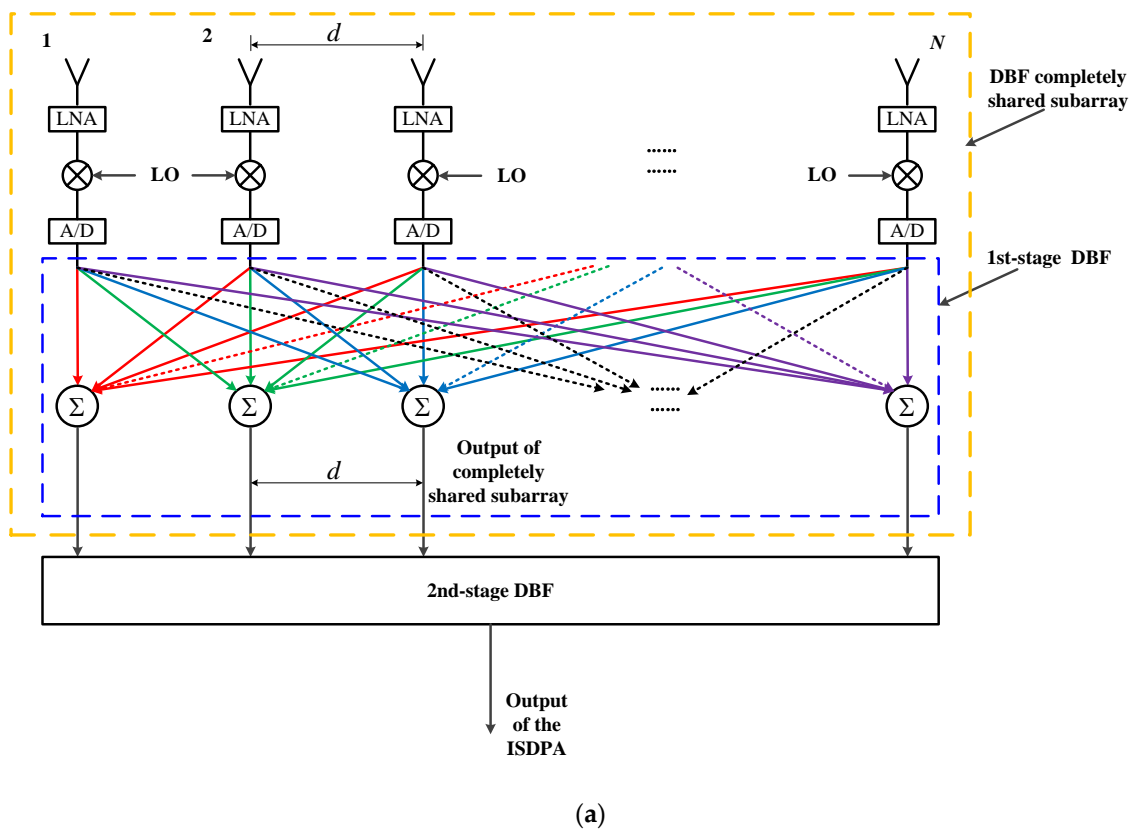


Figure 1. The scheme (a) and geometry (b) of ISDPA based on the DBF completely shared subarray.

Utilizing the DBF completely shared subarray architecture, a novel ISDPA scheme for geostationary satellite applications is proposed in Figure 1a. Each DBF completely shared subarray acts as an equivalent element of the ISDPA. The first-stage DBF performs primary

beamforming to achieve an isoflux beam pattern at the element level. The second-stage DBF then conducts power combining at the subarray level, using weighted values of the shared subarray to enable low sidelobes and beam scanning. For an ISDPA with N DBF completely shared subarrays with phase center spacing d , the pattern with scanning angle θ_0 can be expressed as:

$$E(\theta) = \sum_{n=1}^N A_n^{(2)} e^{j(knd \sin \theta + \varphi_n)} F(\theta) = AF^{(2)}(\theta) \times F(\theta) = AF^{(2)}(\theta) \times AF^{(1)}(\theta) \times f(\theta) \quad (2)$$

where $A_n^{(2)}$ is the excitation coefficient for the n th shared subarray in the second-stage DBF, $\varphi_n = -k \times n \times d \times \sin \theta_0$, and $AF^{(2)}(\theta)$ is the array factor at the subarray level.

For simplicity, we will assume that the radiating antenna element pattern is omnidirectional and focus on optimizing the array factor of the completely shared subarray.

2.2. Goal Pattern and Isoflux Beam Pattern Mask for the DBF Completely Shared Subarray Optimization

The spherical shape of the Earth causes space loss variation between satellites and ground users. Figure 2 shows the geometric model containing a satellite, a ground user, and the Earth. As shown in Figure 2, H is the orbital altitude of the satellite, X is the distance between the satellite and the ground user, R is the radius of the Earth, and θ is the scanning angle of the phased array antenna on the satellite. According to [7], thereby, the relationship between X and the other geometric variables can be written as:

$$R^2 = X^2 + (R + H)^2 - 2X(R + H) \cos(\theta) \quad (3)$$

According to Equation (3), X can be deduced as:

$$X = (H + R) \cos \theta - \sqrt{R^2 - (H + R)^2 \sin^2 \theta} \quad (4)$$

As is known, the space loss between the satellite and the ground user can be written as:

$$\text{SpaceLoss} = 20 \log \left(\frac{4\pi X}{\lambda} \right) \quad (5)$$

Normalized by the satellite orbit altitude H , space loss variation can be obtained as follows:

$$\text{SpaceLoss}_{normalized} = 20 \log \frac{X}{H} = 20 \log \left[\left(1 + \frac{R}{H} \right) \cos \theta - \frac{\sqrt{R^2 - (H + R)^2 \sin^2 \theta}}{H} \right] \quad (6)$$

According to Equation (6), using $H = 36,000$ km for geostationary satellites, Figure 3 shows the normalized space loss variation within $-8^\circ \leq \theta \leq 8^\circ$.

For phased arrays, the element radiation pattern determines scanning gain variation during beam scanning. As an equivalent element of the ISDPA, the completely shared subarray pattern should match the space loss variation within the required scanning range. Therefore, the goal pattern of the completely shared subarray within the required scanning range should be the same as path loss variation. Based on the space loss variation shown in Figure 3, Figure 4 shows the isoflux beam pattern mask with low sidelobes for optimizing the isoflux-shaped beam of the DBF shared subarray. This can be obtained by optimizing the excitation coefficients $\{A_i^{(1)}\}$ for the first-stage DBF using numerical methods, such as the DE algorithm.

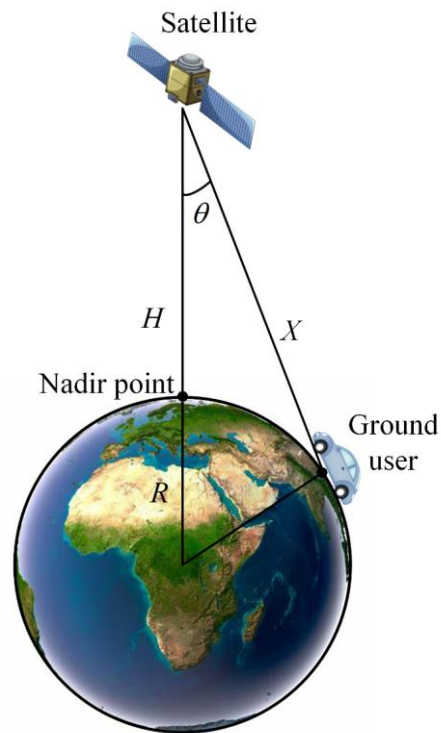


Figure 2. Geometrical model of the satellite, ground user, and the Earth.

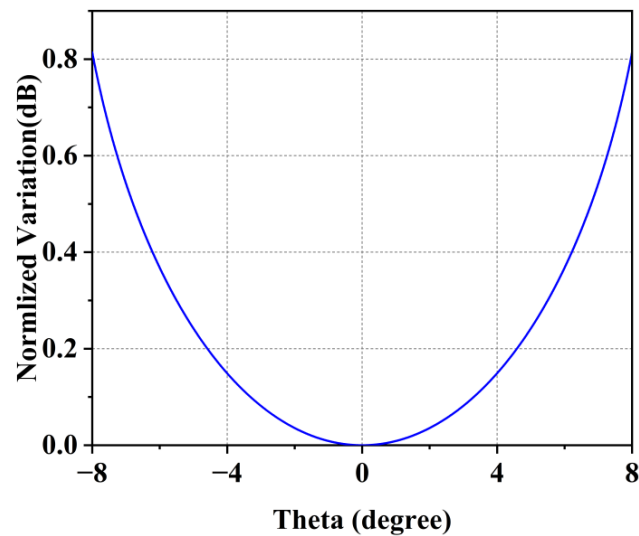


Figure 3. Normalized space loss variation in GEO satellites.

2.3. Design Steps of the ISDPA

Based on the scheme of the ISDPA and goal pattern for the DBF completely shared subarray optimization above, the ISDPA design has the following steps:

- Step 1: Calculate the normalized space loss variation based on the orbit altitude and required scanning range using Equation (6).
- Step 2: Set the sidelobe level of the shared subarray and generate an optimization mask for the shared subarray's isoflux beam pattern $F(\theta)$ based on the normalized space loss variation obtained in step 1.
- Step 3: Use element pattern and a numerical algorithm, e.g., DE algorithm, to optimize the excitation coefficients $\{A_i^{(1)}\}$ of radiating elements in the shared subarray and calculate the optimized shared subarray pattern $F(\theta)$.

- Step 4: Obtain the excitation coefficients $\{A_n^{(2)}\}$ of shared subarrays in the ISDPA by using the Taylor distribution or other methods according to the sidelobe requirements of the ISDPA.
- Step 5: Based on the excitation coefficients $\{A_i^{(1)}\}$ and $\{A_n^{(2)}\}$ obtained from step 3 and step 4, respectively, calculate the radiation patterns at different scanning angles of the ISDPA using Equation (2).

To illustrate the proposed ISDPA optimization mechanism, a flow chart of the process is shown in Figure 5.

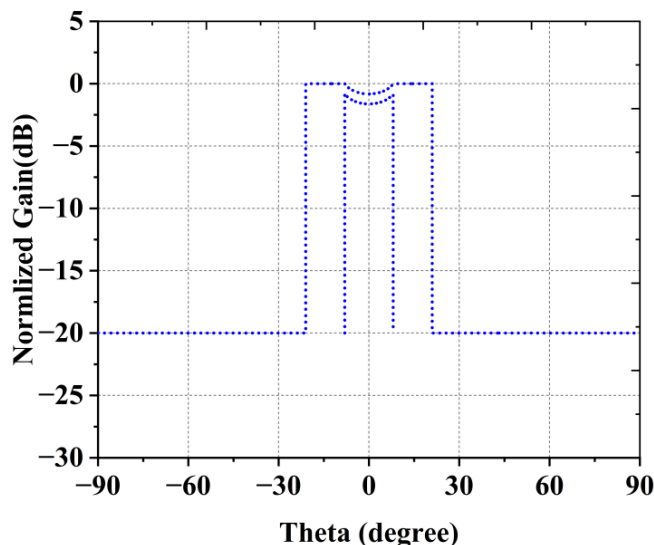


Figure 4. Isoflux beam pattern mask of the DBF shared subarray beam optimization for geostationary satellites.

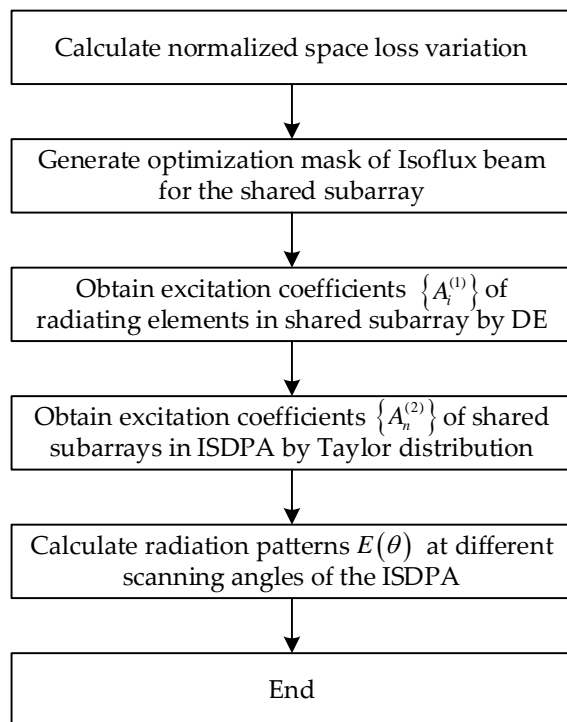


Figure 5. Flow chart of the ISDPA optimization mechanism.

3. Numerical Results and Discussion

3.1. Optimized Results of the DBF Completely Shared Subarray

In this paper, excitation coefficients that generate an isoflux beam pattern for GEO satellites were obtained using the DE algorithm [19] in MATLAB. The analysis considers a linear DBF completely shared subarray of 16 elements with half-wavelength spacing, as shown in Figure 1. The radiating elements in shared subarrays are omnidirectional point-source antennas with omnidirectional radiation patterns. The optimized excitation coefficients and numerically simulated pattern of the DBF completely shared subarray are shown in Table 1 and Figure 6, respectively. Figure 6 also represents the comparison between the optimized isoflux beam pattern and the space loss variation within $-8^\circ \leq \theta \leq 8^\circ$. It can be observed that the optimized isoflux pattern closely matches the space loss variation within this range and has low sidelobe levels better than -20 dB as well.

Table 1. The optimized excitation coefficients of the DBF completely shared subarray.

Element Index	Magnitude (V)	Phase (Degree)
1	0.1093	147.0
2	0.1213	20.0
3	0.2150	4.3
4	0.2765	1.5
5	0.2126	16.0
6	0.2265	93.5
7	0.5755	135.8
8	0.8834	137.1
9	1	146
10	0.9645	138.7
11	0.6246	132.3
12	0.2823	114.5
13	0.2121	36.8
14	0.2755	0
15	0.2588	0.5
16	0.0837	10.9

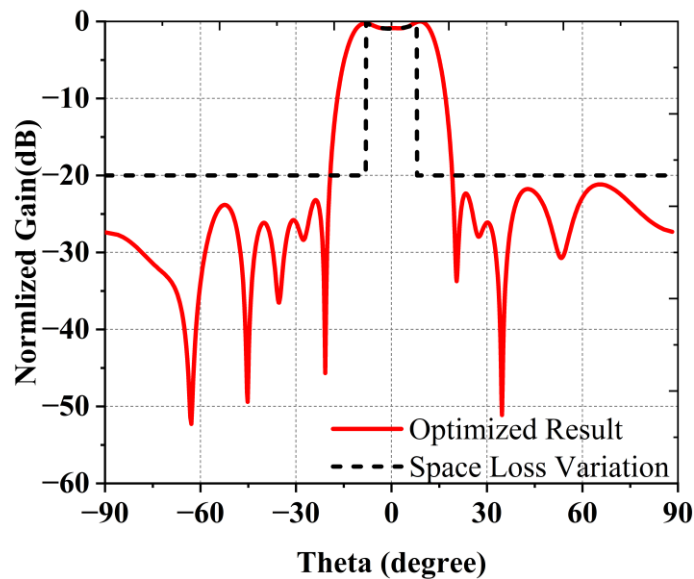
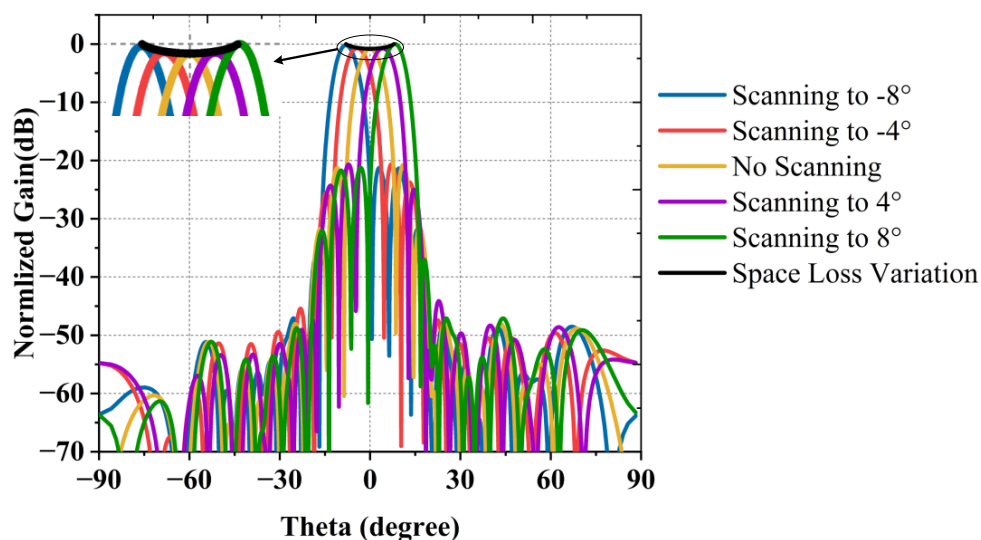


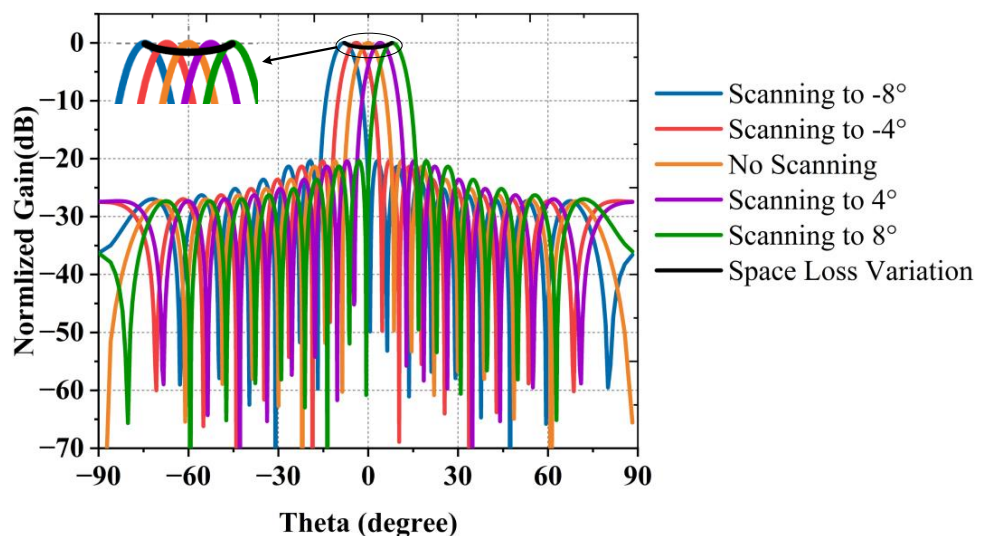
Figure 6. Comparison of optimized isoflux beam pattern and space loss variation for the DBF completely shared subarray.

3.2. Results of the ISDPA

A linear ISDPA with 16 DBF completely shared subarrays is designed, simulated, and analyzed in this work. The distances between both the completely shared subarray phase centers and the radiating elements are half of the wavelength. The ISDPA has two sets of excitation coefficients for the first and second stage of the DBF network: weighted values $\{A_i^{(1)}\}$ optimized using the DE method for an isoflux pattern at the element level in the first stage, and weighted values $\{A_n^{(2)}\}$ with a -20 dB Taylor distribution at the subarray level in the second stage. Using the optimized coefficients $\{A_i^{(1)}\}$ from Table 1 and $\{A_n^{(2)}\}$ with -20 dB Taylor weighting, Figure 7a presents the resultant ISDPA beam scanning characteristics and comparison with space loss variation in MATLAB. Numerical results indicate a maximum 0.13 dB deviation between scanning gain variation and path loss variation, demonstrating the ISDPA's excellent isoflux scanning characteristics.



(a)



(b)

Figure 7. Scanning gain variation during beam scanning compared with space loss variation in the ISDPA (a) and the TLPA (b).

To compare the differences in beam scanning gain variation between the ISDPA and traditional phased array antenna, a traditional linear phased array (TLPA) composed of 16 elements with an omnidirectional radiation pattern arranged according to Figure 1b is designed and analyzed. The TLPA elements have a spacing of 0.5λ and share the same excitation coefficients as the second-stage excitation coefficients $\{A_n^{(2)}\}$ used in the ISDPA. Simulation results comparing the gain variation characteristics during beam scanning with the space loss variation are shown in Figure 7b and Table 2, respectively. From Figure 7, it can be observed that, compared to the TLPA, which cannot achieve a matched variation between scanning gain and space loss, the scanning gain of the ISDPA is minimized in the nadir direction without scanning, ascending with the increase in the beam scanning angle, and it exhibits no grating lobes and a low sidelobe level performance better than -20 dB, improving the interference rejection in the satellite communication system.

Table 2. Performance comparison between this work and the references for GEO satellites.

Reference	Architecture	Aperture	Gain Variation Follows the Space Loss Variation	Electrically Beam Scanning	Sidelobe Level	Max Deviation between Scanning Gain Variation and Space Loss Variation
[12]	Non-shared subarray	7.2λ	Yes	No	-14 dB	-
[15]	Non-shared subarray	6λ	Yes	No	-17 dB	-
TLPA in this work	Non-shared subarray	8λ	No	Yes	≤ -20 dB	0.81 dB
ISDPA in this work	Shared subarray	8λ	Yes	Yes	≤ -20 dB	0.13 dB

Finally, a performance comparison between this work and related work for GEO satellite applications is shown in Table 2. It is evident that the scanning gain variation in the proposed ISDPA follows the space loss variation during electrical beam scanning with low sidelobes, demonstrating isoflux scanning characteristics and enabling a constant communication link in satellite communications.

4. Conclusions

This paper proposed an innovative isoflux scanning digital phased array antenna (ISDPA) design based on a DBF completely shared subarray architecture. A new method to obtain an isoflux beam pattern employing a DBF completely shared subarray and the DE algorithm was presented, optimized, and analyzed. The numerical results indicated that the novel proposed ISDPA is characterized by isoflux scanning, low sidelobe performance, and no grating lobes during beam scanning for geostationary satellite applications.

Author Contributions: Conceptualization, M.C. and Y.L.; methodology, M.C., W.L. and X.S.; software, M.C.; validation, Q.Z. and H.L.; formal analysis, M.C.; investigation, M.C.; resources, M.C.; data curation, M.C.; writing—original draft preparation, M.C.; writing—review and editing, W.L.; visualization, M.C.; supervision, X.S. All authors have read and agreed to the published version of the manuscript.

Funding: This research was funded by the National Key Research and Development Program of China under No. 2019YFB1803200.

Data Availability Statement: Please contact Muren Cai at mr_cai2012@126.com.

Conflicts of Interest: The authors declare no conflict of interest.

References

1. Maral, G.; Bousquet, M.; Sun, Z. *Satellite Communications Systems: Systems, Techniques and Technology*, 6th ed.; John Wiley & Sons: Hoboken, NJ, USA, 2020; pp. 49–55.
2. Wu, R.; Yang, F. Study on Key Technique and Research Hotspot of Low Orbit Satellite Communication. In Proceedings of the 2021 International Conference on Wireless Communications and Smart Grid (ICWCSG), Hangzhou, China, 13–15 August 2021; pp. 89–93.
3. Yuxuan, G.; Yue, L.; Penghui, S. Research Status of Typical Satellite Communication Systems. In Proceedings of the 2021 19th International Conference on Optical Communications and Networks (ICOON), Qufu, China, 23–27 August 2021; pp. 1–3.
4. Al-Hraishawi, H.; Chougrani, H.; Kisseleff, S.; Lagunas, E.; Chatzinotas, S. A Survey on Nongeostationary Satellite Systems: The Communication Perspective. *IEEE Commun. Surv. Tutor.* **2023**, *25*, 101–132. [[CrossRef](#)]
5. Yu, L.; Wan, J.; Zhang, K.; Teng, F.; Lei, L.; Liu, Y. Spaceborne Multibeam Phased Array Antennas for Satellite Communications. *IEEE Aerosp. Electron. Syst. Mag.* **2023**, *38*, 28–47. [[CrossRef](#)]
6. Li, W.; Yu, X.; Chen, P. Left-Hand Circularly Polarized Phased Array with High Gain for Mobile Satellite Communications. In Proceedings of the 2021 IEEE 4th International Conference on Electronic Information and Communication Technology (ICEICT), Xi'an, China, 18–20 August 2021; pp. 227–230.
7. Luu, Q.; Zhu, A.; Abdelrahmanline, A.H.; Ballou, M. Ka Band Phased Array Development Platform. In Proceedings of the 2022 IEEE International Symposium on Phased Array Systems & Technology (PAST), Waltham, MA, USA, 11–14 October 2022; pp. 1–6.
8. Akan, V. Design of Polyrod Antenna Having Isoflux Radiation Characteristic for Satellite Communication Systems. *Int. Adv. Res. Eng. J.* **2020**, *4*, 226–232. [[CrossRef](#)]
9. Arnaud, E.; Dugenet, J.; Elis, K.; Girardot, A.; Guihard, D.; Menudier, C.; Monediere, T.; Roziere, F.; Thevenot, M. Compact Isoflux X-Band Payload Telemetry Antenna with Simultaneous Dual Circular Polarization for LEO Satellite Applications. *Antennas Wirel. Propag. Lett.* **2020**, *19*, 1679–1683. [[CrossRef](#)]
10. Caminita, F.; Martini, E.; Minatti, G.; Sabbadini, M.; Maci, S. Low-Profile Dual-Polarized Isoflux Antennas for Space Applications. *IEEE Trans. Antennas Propag.* **2021**, *69*, 3204–3213. [[CrossRef](#)]
11. Minatti, G.; Maci, S.; De Vita, P.; Freni, A.; Sabbadini, M. A Circularly-Polarized Isoflux Antenna Based on Anisotropic Metasurface. *IEEE Trans. Antennas Propag.* **2012**, *60*, 4998–5009. [[CrossRef](#)]
12. Ibarra, M.; Reyna, A.; Panduro, M.A.; del Rio-Bocio, C. Design of aperiodic planar arrays for desirable isoflux radiation in GEO satellites. In Proceedings of the 2011 IEEE International Symposium on Antennas and Propagation (APSURSI), Spokane, WA, USA, 3–8 July 2011; pp. 3003–3006.
13. Diener, J.E.; Jones, R.D.; Elsherbeni, A.Z. Isoflux Phased Array Design for Cubesats. In Proceedings of the 2017 IEEE International Symposium on Antennas and Propagation & USNC/URSI National Radio Science Meeting, San Diego, CA, USA, 9–15 July 2017; pp. 1811–1812.
14. Li, S.; Liao, S.; Yang, Y.; Che, W.; Xue, Q. Low-Profile Circularly Polarized Isoflux Beam Antenna Array Based on Annular Aperture Elements for CubeSat Earth Coverage Applications. *IEEE Trans. Antennas Propag.* **2021**, *69*, 5489–5502. [[CrossRef](#)]
15. Mukherjee, A.; Kumar, S.S.; Singhal, A.K. A Thinned Array Solution for an ISOFLUX Antenna from Geostationary Satellite. In Proceedings of the 2018 IEEE Indian Conference on Antennas and Propagation (InCAP), Hyderabad, India, 16–19 December 2018; pp. 1–6.
16. Bianchi, D.; Genovesi, S.; Monorchio, A. Randomly Overlapped Subarrays for Reduced Sidelobes in Angle-Limited Scan Arrays. *Antennas Wirel. Propag. Lett.* **2017**, *16*, 1969–1972. [[CrossRef](#)]
17. An, Q.; Yeh, C.; Lu, Y.; He, Y.; Yang, J. A Convex Optimization Based Multistage Wideband Pattern Accurate Synthesis Method for Overlapping Subarrays. *Signal Process.* **2023**, *213*, 109197. [[CrossRef](#)]
18. Li, X.-X.; Dong, W.; Xu, Z.-H.; Xiao, S.-P. Hierarchical Array Design Strategy Composed of Irregular and Overlapped Subarrays in Large-Scale Planar Array. *IEEE Trans. Antennas Propag.* **2021**, *69*, 4217–4222. [[CrossRef](#)]
19. Bilal; Pant, M.; Zaheer, H.; Garcia-Hernandez, L.; Abraham, A. Differential Evolution: A Review of More than Two Decades of Research. *Eng. Appl. Artif. Intell.* **2020**, *90*, 103479. [[CrossRef](#)]

Disclaimer/Publisher's Note: The statements, opinions and data contained in all publications are solely those of the individual author(s) and contributor(s) and not of MDPI and/or the editor(s). MDPI and/or the editor(s) disclaim responsibility for any injury to people or property resulting from any ideas, methods, instructions or products referred to in the content.